

## Electrical transport in junctions between unconventional superconductors: Application of the Green's-function formalism

Manoj P. Samanta\* and Supriyo Datta

*School of Electrical and Computer Engineering and the MRSEC for Technology Enabling Heterostructure Materials, Purdue University,  
West Lafayette, Indiana 47907-1285*

(Received 28 July 1997; revised manuscript received 6 November 1997)

We present a general Green's-function-based method that can be used to describe the electrical transport properties of junctions with arbitrary coupling strength involving superconductors with unconventional pairing symmetry and arbitrary band structures. Our method correctly takes into account the midgap surface states that arise in  $d$ -wave superconductors due to sign change of the order parameter. In the tunneling limit, we present simple expressions that describe the effect of the midgap states on the dc and ac components of the Josephson current including their temperature dependence. A numerical example is presented for a junction between two  $d$ -wave superconductors with arbitrary coupling strength showing a feature originating from the sign change of the order parameter, namely, for some orientations of the  $d$ -wave order parameter relative to the surface, the current-phase relation may remain nonsinusoidal even when the coupling is quite weak.

[S0163-1829(98)03217-2]

### I. INTRODUCTION

It is by now well known that the electrical transport properties of unconventional superconductors are qualitatively different from the conventional  $s$ -wave superconductors. For example, the change in sign of the order parameter in  $d$ -wave superconductors gives rise to effects such as midgap surface states<sup>1-9</sup> that do not have any analog for  $s$ -wave superconductors. Therefore, in modeling junctions between unconventional superconductors, a straightforward generalization of the existing methods for the  $s$ -wave superconductors is not possible. In this paper, we present a general and powerful numerical method to model junctions between unconventional superconductors that correctly accounts for the surface effects. Our method can easily include any unconventional pairing symmetry, arbitrary coupling strength and band structures (Sec. II) and therefore will be useful in comparing theory and experiment for junctions between high-temperature superconducting (HTSC) materials. In the tunneling limit, our method gives simple expressions including temperature dependence for the dc Josephson current, the ac Josephson current, and the quasiparticle current (Sec. III) which provide greater insight than a purely numerical calculation based on the full theory.<sup>9</sup> These general expressions can be used for any unconventional pairing symmetry such as  $d+s$ ,  $d$ ,  $d+id$ ,  $s+id$ , etc., and provide unified understanding of a wide class of anomalous phenomena. The expression for the quasiparticle current explains all the tunneling limit features due to midgap states discussed in Ref. 9 with simple "back-of-the-envelope" calculations. In addition, it predicts other features that were not discussed in Ref. 9, such as negative conductance near zero bias for a junction between two  $d$ -wave superconductors. Moreover, the temperature dependence of all these features are included in our expression, whereas the calculation in Ref. 9 is only at zero temperature. The expression for the dc Josephson current shows the  $\sin 2\theta_1 \sin 2\theta_2$  angular dependence ( $\theta_1$  and  $\theta_2$  being

the misorientation angles of the  $d$ -wave superconductors) and  $1/T$  temperature dependence of the midgap component of the Josephson current. This result is used in Ref. 5 to predict the effect of midgap states on the flux quantization in the tricrystal ring experiment.<sup>10</sup> In Sec. IV, we present a numerical example illustrating a feature originating from the sign change of the order parameter. Unlike  $s$ -wave junctions, where the current phase relation  $[I(\phi)]$  changes from nonsinusoidal to sinusoidal dependence as the coupling is reduced, for some orientations of the  $d$ -wave order parameter  $I(\phi)$  may remain nonsinusoidal even for weakly coupled junctions.<sup>11</sup> Some evidence of similar behavior has been seen experimentally<sup>12</sup> and our theory should provide motivation for further experiments in this direction.

In the context of low- $T_c$  superconductors, the scattering theory<sup>13-18</sup> of transport has been fairly successful in describing junctions between two superconductors with arbitrary coupling. This method has recently been extended to superconductors with unconventional order parameter symmetry.<sup>2,4,9</sup> Although the scattering formalism is conceptually simple, it is difficult to apply it to complicated geometries or to include arbitrary spatial variations and band structures because of the need to calculate the precise eigenstate spectrum. The nonequilibrium Green's-function (NEGF) formalism provides a more general framework for the treatment of electrical transport in superconducting junctions. It has been applied successfully to junctions between  $s$ -wave superconductors.<sup>19,20</sup> In this paper we extend the NEGF method to unconventional superconductors by properly including the surface effects such as midgap states arising from the sign change of the order parameter. We use a tight-binding description which can handle unconventional pairing symmetry and also include arbitrary band structures if necessary. In the absence of dephasing processes, NEGF formalism is equivalent to the scattering method and yields identical answers. This equivalence has been shown in Ref. 21 for normal conductors and the proof can be extended for

superconductors in a straightforward manner. Compared to scattering theory, the advantage of the NEGF based method presented here lies in the ease with which it can handle various surface-related complexities which play a significant role in HTSC junctions. Also it should be noted that we do not use the quasiclassical (Andreev) approximation (coherence length much larger than the Fermi wavelength) used in the quasiclassical Green's-function method,<sup>6,22-25</sup> which is of reduced validity in HTSC's due to their substantially shorter coherence length.<sup>22</sup> We believe the method presented here will be helpful in performing detailed quantitative comparisons with experiments on HTSC junctions.

## II. THEORETICAL FORMULATION

In this section we present our method for computing the dc and ac components of the current  $I$  for a bias  $V$  across a junction between two unconventional superconductors. The discussion in this section is completely general and specific cases are considered in Secs. III and IV. We start from the Bogoliubov-de Gennes (BdG) equation<sup>26</sup> [Eq. (2)] to model the superconductors and compute the current as follows: (a) We compute the retarded Green's function ( $G$ ) from the  $2 \times 2$  BdG Hamiltonian in Eq. (2) (Sec. II B).  $G$  contains the same physics that is described by the wave functions in the scattering approach. (b) We compute the correlation function  $G^<$  from  $G$  using the NEGF formalism<sup>21,27</sup> (Sec. II C). (c) We obtain all quantities of interest such as the electron density and the current from  $G^<$  (Sec. II D).

In this paper, we represent the BdG equation on a discrete tight-binding lattice. One advantage of choosing discrete tight-binding representation is that arbitrary band structure<sup>28</sup> and pairing symmetry can be modeled by choosing suitable matrices to represent the Hamiltonian  $H$  and the pair potential  $\Delta$  [see Eq. (2)]. The specific example in Sec. IV shows how we model a  $d$ -wave pair potential in tight-binding form.

### A. Outline

We consider a planar structure consisting of a normal device region sandwiched between two uniform semi-infinite superconducting leads (1 and 2) [Fig. 1(a)]. Our aim is to compute the current  $I$  for a potential difference  $V$  between the leads [see potential profile in Fig. 1(a)]. When both the leads are superconducting, a dc voltage  $V$  applied between the leads gives rise to an ac current<sup>17,19,20,29</sup>

$$I(t) = \sum_{k=-\infty}^{\infty} I_k e^{ik\omega_0 t}, \quad (1)$$

where  $\omega_0 = 2eV/\hbar$  is the Josephson frequency. In Eq. (1),  $I_{-k} = I_k^*$  for the current to be real. Our objective is to calculate the different  $I_k$  for a given  $V$ .

Quasiparticle motion in this structure is described by the Bogoliubov-de Gennes equation<sup>18,26</sup> given as

$$i\hbar \frac{\partial}{\partial t} \begin{bmatrix} \Psi^e \\ \Psi^h \end{bmatrix} = \begin{bmatrix} (H + U - \mu_F) & \Delta e^{-2i\mu t/\hbar} \\ \Delta^\dagger e^{2i\mu t/\hbar} & -(H^* + U - \mu_F) \end{bmatrix} \begin{bmatrix} \Psi^e \\ \Psi^h \end{bmatrix}. \quad (2)$$

Physically Eq. (2) describes the motion of up-spin electrons and down-spin holes coupled together.<sup>18</sup> The Eilenberger equation, used alternatively as a starting point in the

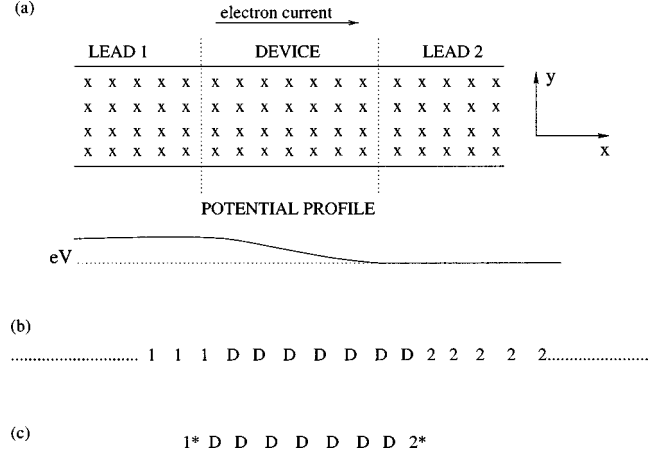


FIG. 1. (a) A structure consisting of a normal device region connected between two uniform semi-infinite superconducting leads. We model it in the discrete space, where the structure is represented by set of lattice points marked as X in the figure. A voltage  $V$  is applied between the leads. The given potential profile for the system is also shown. (b) Conceptually (a) is equivalent to a one-dimensional layer of lattice points, where the device is represented by a finite set of lattice points marked  $D_i$ , while contacts 1 and 2 are represented by infinite set of lattice points marked as 1 and 2, respectively. Each point  $D_i$ , 1, and 2 represents a layer of the structure. (c) The semi-infinite contacts can be effectively modeled by the single points  $1^*$  and  $2^*$ , that take the effect due to the whole contact correctly into account.

literature,<sup>6,22-25</sup> is an approximate form of Eq. (2) valid only in the quasiclassical limit. In Eq. (2),  $H$  is the one-electron Hamiltonian and  $\Delta$  is the operator representing the pair potential (order parameter) including the phase of the superconductor; it is zero in the normal device region. The reference potential  $\mu_F$  is constant everywhere.  $U$  is the electrostatic potential as shown in Fig. 1(b); it is constant in the superconducting leads but spatially varying in the device region.  $\mu$  is the chemical potential with respect to the reference level  $\mu_F$ .  $\mu$  is constant in the superconducting leads 1 and 2 equal to  $\mu_1$  and  $\mu_2$ , respectively, with  $\mu_1 - \mu_2 = eV$ . The normal region may be significantly out of equilibrium and may not have any well-defined chemical potential  $\mu$ . However, this does not matter since  $\Delta$  is zero anyway. In our formulation, we start with given  $H$ ,  $U$ ,  $\mu$ ,  $\Delta$ ,  $\mu_F$ , and compute the current. In a complete calculation both  $U$  and  $\Delta$  need to be computed self-consistently.<sup>6,22,26</sup> However the self-consistency equation for  $U$  and  $\Delta$  depends on the microscopic theory for the pairing interaction and represents a separate story that we will not consider in this paper.

For our computation we work in the energy domain rather than the time domain [Eq. (2)], starting from an equation which is the Fourier transform of Eq. (2). Although ideally the energy ranges from  $-\infty$  to  $\infty$ , sufficient numerical accuracy can be achieved at low bias by considering the energy values within a few multiples of the maximum superconducting gap. We consider an energy range ( $E_{\min}, E_{\max}$ ) and discretize it in  $N_E$  points. Also we discretize the system in real space [Fig. 1(a)]. We consider  $N_x$  and  $N_y$  points in the device in the  $x$  and  $y$  directions, respectively. The leads have infinite number of points in the  $x$  direction and  $N_y$  points in the  $y$  direction. All operators in our formulation are matrices

having matrix elements between every  $(x_1, y_1, E_1, s_1)$  and  $(x_2, y_2, E_2, s_2)$  where  $(x_i, y_i, E_i, s_i)$  represents  $(x$  coordinate,  $y$  coordinate, energy, spin) of a point. Band indices are implicitly included in  $y_i$ .

### B. Retarded Green's function

The retarded Green's function  $G$  is defined as

$$G = (E^M - H^{\text{BdG}} + i\eta)^{-1}, \quad (3)$$

where

$$E^M(x_1, y_1, E_1, s_1, x_2, y_2, E_2, s_2) = E_1 \delta_{E_1, E_2} \delta_{x_1, x_2} \delta_{y_1, y_2} \delta_{s_1, s_2}$$

and  $H^{\text{BdG}}$  is the energy domain representation of the time-dependent BdG Hamiltonian in Eq. (2).  $\delta_{a,b}$  is the Kronecker delta function which is 1 if  $a=b$  and 0 if  $a \neq b$ . Since we are considering an open system consisting of semi-infinite leads, the matrix on the right-hand side of Eq. (3) is of infinite dimension and cannot be inverted directly. In the literature this problem is often avoided by using periodic boundary condition. However, this would give rise to a discrete spectrum rather than a continuous spectrum appropriate for an open system. In this paper we take the infinite leads correctly into account following a procedure initiated by Caroli for normal conductors.<sup>30</sup> We are not interested in the Green's function inside the contacts. Therefore, we define an "effective device" consisting of the given device region and also one extra layer from each lead immediately connecting the device [layers 1\* and 2\* in Fig. 1(c)], and compute only the part of  $G$  for this region [ $G_D$ ] using the following equation that can be derived from Eq. (3):<sup>31</sup>

$$G_D = \begin{bmatrix} g_1^{-1} & -\tau_1 & 0 \\ -\tau_1^\dagger & g_D^{-1} & -\tau_2 \\ 0 & -\tau_2^\dagger & g_2^{-1} \end{bmatrix}^{-1}. \quad (4)$$

In Eq. (4), rows (columns) 1, 2, and 3 correspond to layer 1\*, device region, and layer 2\* respectively. Therefore  $g_D$  is the retarded Green's function of the isolated device region.  $\tau_i$  is the coupling between the device and the layer  $i^*$  obtained from  $H^{\text{BdG}}$ .  $g_i$  is the surface Green's function for the isolated lead  $i$  on the layer  $i^*$ . We describe a procedure to compute it in the following paragraph.  $G_D$  in Eq. (4) is a matrix of dimension  $2(N_x + 2)N_y N_E$ . If  $g_1$  and  $g_2$  are calculated correctly,  $G_D$  is exact. Our method is numerically efficient since for different systems with identical leads the lead Green's functions need to be computed only once and saved for reuse.

The surface Green's function  $g_i$  in Eq. (4) is the value of the lead Green's function  $G_i$  at the surface layer  $i^*$ .  $G_i$  is obtained from an equation similar to Eq. (3) with  $H^{\text{BdG}}$  replaced by the Hamiltonian for the isolated lead. The Hamiltonian of a superconducting lead has nonzero matrix elements between different energies [check the Fourier transform of the Hamiltonian in Eq. (2)] and so  $G_i(E_1, E_2)$  is computed in two steps. Since the lead has constant chemical potential  $\mu_i$ , the lead Hamiltonian is first locally gauge transformed to an energy-independent form (denoted by an overline). The Green's function of this energy-independent Hamiltonian is computed from

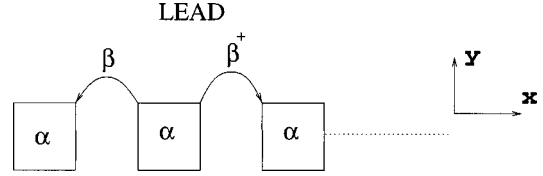


FIG. 2. Since each of the lead is uniform, the lead Hamiltonian can be described by two terms—the Hamiltonian matrix for each layer ( $\alpha$ ) and the matrix representing the coupling between two neighboring layers ( $\beta$ ). Arbitrary band structures and pair potentials in the lead can be modeled by choosing appropriate  $\alpha$  and  $\beta$ .

$$\begin{aligned} \bar{G}_i(E) &= \begin{bmatrix} \bar{G}_i^{ee}(E) & \bar{G}_i^{eh}(E) \\ \bar{G}_i^{he}(E) & \bar{G}_i^{hh}(E) \end{bmatrix} \\ &= \begin{bmatrix} (E + i\eta)I - H_L + \mu_F & -\Delta \\ -\Delta^\dagger & (E + i\eta)I + H_L^* - \mu_F \end{bmatrix}_{\eta \rightarrow 0}^{-1}, \end{aligned} \quad (5)$$

where  $H_L$  and  $\Delta$  are the single-electron Hamiltonian and the pair potential in the lead.  $\bar{G}_i(E)$  is transformed back to the energy-dependent  $G_i(E_1, E_2)$  using

$$\begin{aligned} G_i^{ee}(E', E) &= \delta_{E', E} \bar{G}_i^{ee}(E - \mu_i), \\ G_i^{eh}(E', E) &= \delta_{E', E + 2\mu_i} \bar{G}_i^{eh}(E + \mu_i), \\ G_i^{he}(E', E) &= \delta_{E', E - 2\mu_i} \bar{G}_i^{he}(E - \mu_i), \\ G_i^{hh}(E', E) &= \delta_{E', E} \bar{G}_i^{hh}(E + \mu_i). \end{aligned} \quad (6)$$

When  $\mu_i$  is zero, these transformations are not necessary.

Since the lead Hamiltonian is infinite, the inversion in Eq. (5) cannot be done directly. For  $s$ -wave superconductors this is not necessary, because the surface Green's function is equal to the bulk Green's function (Green's function of an infinite lead) that can be obtained easily by other methods.<sup>20</sup> However, for unconventional superconductors, the surface Green's function can be qualitatively different from the bulk Green's function. Here we present a general method to compute the surface Green's function for any arbitrary superconductor. We note that in Eq. (4) we only need  $g_i$  rather than the whole  $G_i$ , and therefore we do not need to invert the infinite Hamiltonian matrix for the lead. Since we have assumed the lead to be uniform throughout its length, the Hamiltonian for the lead can be written in terms of just two matrices—the Hamiltonian for each layer ( $\alpha_i$ ) and the Hamiltonian coupling successive layers ( $\beta_i$ ) (Fig. 2). To compute  $g_i(E_1, E_2)$ , we first solve for the energy-independent  $\bar{g}_i(E)$  from

$$\bar{g}_1(E) = [(E + i\eta)I - \alpha_1 - \beta_1^\dagger \bar{g}_1(E) \beta_1]_{\eta \rightarrow 0}^{-1}, \quad (7)$$

$$\bar{g}_2(E) = [(E + i\eta)I - \alpha_2 - \beta_2 \bar{g}_2(E) \beta_2^\dagger]_{\eta \rightarrow 0}^{-1}, \quad (8)$$

using an iterative procedure (see Appendix B1) and then use transformations as given by Eq. (6).

### C. Correlation functions

In order to compute the current, it is enough to know the part of the correlation function for the ‘‘effective device’’ region [ $G_D^<$ ]. In equilibrium ( $V=0$ ) the system is described by a single chemical potential. If we choose it to be equal to the reference potential  $\mu_F$ ,  $G_D^<$  is related to  $G_D$  by<sup>21,27</sup>

$$G_D^< = (G_D^\dagger - G_D)f(E), \quad (9)$$

where  $f$  is the Fermi function. In the presence of nonzero applied bias  $V$ , the device region does not have any well-defined chemical potential and therefore we need to use NEGF formalism<sup>21,27</sup> to obtain the following relation between  $G_D^<$  and  $G_D$ :

$$G_D^< = G_D \Sigma_D^< G_D^\dagger, \quad (10)$$

where

$$\Sigma_D^< = \begin{bmatrix} \sigma_1^< & 0 & 0 \\ 0 & 0 & 0 \\ 0 & 0 & \sigma_2^< \end{bmatrix}. \quad (11)$$

Similar to Eq. (4), rows (columns) 1, 2, and 3 in Eq. (11) correspond to layer 1\*, device region, and layer 2\*, respectively. The quantities  $\sigma_1^<$  and  $\sigma_2^<$  represent the in-scattering functions from leads 1 and 2, respectively, and depend on the respective chemical potentials.  $\sigma_i^<$  has matrix elements coupling different energies similar to  $g_{is}$ 's in the previous subsection. Therefore using the fact that the leads are locally in equilibrium with constant chemical potential  $\mu_i$ , the in-scattering functions in the transformed domain are given by

$$\begin{aligned} \bar{\sigma}_1^<(E) &= f(E)\beta_1^\dagger[\bar{g}_1^\dagger(E) - \bar{g}_1(E)]\beta_1, \\ \bar{\sigma}_2^<(E) &= f(E)\beta_2[\bar{g}_2^\dagger(E) - \bar{g}_2(E)]\beta_2^\dagger. \end{aligned} \quad (12)$$

To return to the untransformed representation, we use Eq. (6) with  $g$  replaced by  $\sigma_{1,2}^<$ . Since two leads have different  $\mu_i$ 's, they will be transformed back differently. This is where the effect due to the applied potential  $V$  is being taken into account.

### D. Current operator

In our formulation, all the different components of the current can be obtained from the current operator defined in terms of the correlation function as<sup>32</sup>

$$\begin{aligned} I_{\text{op}} &= \frac{e}{h} [H_D^{\text{BdG}}(x_i, x_{i+1}) G_D^<(x_{i+1}, x_i) \\ &\quad - G_D^<(x_i, x_{i+1}) H_D^{\text{BdG}}(x_{i+1}, x_i)], \end{aligned} \quad (13)$$

where  $x_i$  and  $x_{i+1}$  represent points in the adjacent layers of the device in the  $x$  direction. We use the notation  $G_D(x_i, x_{i+1})$  to indicate part of  $G_D$  coupling  $x_i$  and  $x_{i+1}$  (i.e., layers  $i$  and  $i+1$ ) that includes all  $y_i$ 's,  $E_i$ 's, and spins. Therefore, the current operator is a square matrix of dimension  $2N_y N_E$  with terms as  $I_{\text{op}}(y_1, E_1, s_1, y_2, E_2, s_2)$ , where  $y = (1, N_y)$ ,  $E = (1, N_E)$ ,  $s = (e, h)$ . Different current compo-

nents in Eq. (1) are given by the elements of the current-operator diagonal or off-diagonal in the energy space:

$$I_k(V) = 2 \frac{\Delta E}{N_y} \sum_{y, E} [I_{\text{op}}(y, E - k\hbar\omega_0, e, y, E, e)], \quad (14)$$

where  $\Delta E = (E_{\text{max}} - E_{\text{min}})/N_E$ .  $I_k(V)$  in Eq. (14) is expressed in terms of current or mode. Electron-hole symmetry is used to simplify Eq. (14).

## III. TUNNELING LIMIT

One advantage of the Green's function based method presented in Sec. II over scattering theory is that the expression for current simplifies significantly for weakly coupled ‘‘tunnel’’ junctions. Such weakly coupled junctions have been studied extensively in the context of low- $T_c$  superconductors, but in the present context they are particularly relevant. This is because the effect of the midgap states is most prominent for weakly coupled junctions, whose  $I$ - $V$  characteristics can be modeled with a much simpler first order theory that provide greater insight than a purely numerical calculation based on the full theory.<sup>9</sup> In this section, we present such a theory which could be described as a generalized tunneling Hamiltonian formalism. Expanding the Green's functions of Sec. II in perturbation series and keeping only the first order terms, simple expressions for the dc Josephson current [Eq. (16)], first harmonic [Eq. (18)], and the quasiparticle current [Eq. (17)] are obtained. Equations (16)–(18) are very general and can be applied for superconductors with any unconventional pairing symmetry ( $d$ ,  $d+id$ ,  $s+id$ , etc.) providing a unified understanding of a wide class of observable anomalies associated with the unconventional order parameter. For a tunnel junction between a normal metal and a  $d$ -wave superconductor, the expression for the quasiparticle current [Eq. (17)] reproduces the theory of midgap states given in Ref. 2. When one or both of the superconductors have  $d$ -wave symmetry, it provides a simple explanation for the features due to midgap states obtained in Ref. 9 from full calculation based on scattering theory. Additionally, it predicts other features in the  $I$ - $V$  characteristics such as negative conductance near zero bias that were not discussed in Ref. 9. Moreover, the temperature dependence of all these features can be obtained from the same expression, whereas the calculation in Ref. 9 is only at zero temperature. The expression for the dc Josephson current [Eq. (16)] shows the  $\sin 2\theta_1 \sin 2\theta_2$  angular dependence and  $1/T$  temperature dependence of the midgap component of the Josephson current. This result is used in Ref. 5 to predict effect of midgap states on the flux quantization in the tricrystal experiment.<sup>10</sup>

For  $s$ -wave junctions, Eqs. (15)–(18) reduce to the conventional tunneling Hamiltonian expressions.<sup>33</sup> For example, the quasiparticle current  $i_{\text{QP}}$  is expressed as the product of the density of states (DOS) for the two electrodes (note that  $\text{DOS} = a^{ee}$ ), while the dc and ac Josephson currents  $i_J$  and  $i_1$  are expressed as the product of the pair correlation functions  $\bar{g}^{eh}$  and  $\bar{g}^{eh}$ . The main difference for unconventional superconductors is simply that all the quantities appearing in our expressions represent surface quantities while it is customary to use bulk quantities. For  $s$ -wave superconductors this is not an issue, since the surface and bulk Green's functions have

essentially the same functional form. However, for unconventional superconductors whose pair potential changes sign in different directions, the surface and bulk Green's functions can be qualitatively different. Depending on the surface orientation, the former could show midgap peaks that are absent in the bulk Green's function and it is these midgap peaks that are responsible for diverse anomalies such as the unusual temperature dependence and  $\sin 2\theta_1 \sin 2\theta_2$  angular dependence of Josephson current and negative differential conductance. All these phenomena are understood easily from Eqs. (16)–(18) if we use the surface Green's function, but *not* if we use the bulk Green's function.

We consider a short tunnel junction between two unconventional superconductors, where the coupling between the superconductors is given by tunneling matrix element  $M$ . Starting from the general theory in Sec. II, expanding the Green's functions in powers of  $M$  and keeping only the first order terms (derivation given in Appendix A), we obtain the following equations for the dc component  $I_0$  and the first harmonic  $I_1$  of the current (note that  $I_{-1} = I_1^*$ ):

$$I_{0,1}(V) = \frac{e}{h} \int_{-\infty}^{\infty} dE \int_{-\infty}^{\infty} \frac{dk_y}{2\pi} |M(k_y)|^2 i_{0,1}(E, k_y, V). \quad (15)$$

The dc term  $i_0$  is given by the sum of a zero-bias dc Josephson component  $i_J$  and a quasiparticle component  $i_{QP}$  (present under bias):

$$i_J(E, k_y) = 4 \operatorname{Re} [\bar{g}_1^{he}(E, k_y) \bar{g}_2^{eh}(E, k_y) - \bar{g}_2^{he}(E, k_y) \bar{g}_1^{eh}(E, k_y)] f(E), \quad (16)$$

$$i_{QP}(E, k_y, V) = 2 [\bar{a}_2^{ee}(E+V, k_y) \bar{a}_1^{ee}(E, k_y)]$$

$$[f(E) - f(E+V)] \quad (17)$$

while the first harmonic is given by

$$i_1(E, k_y) = -2i [\bar{a}_2^{eh}(E, k_y) \{\bar{g}_1^{eh}(E+V, k_y)^*\} + \bar{a}_1^{he}(E, k_y) \times \{\bar{g}_2^{eh}(E-V, k_y)\}] f(E). \quad (18)$$

All higher harmonics are zero to this order. We have assumed the structure to be uniform in the  $y$  direction so that solutions with different  $k_y$  are decoupled and their contributions to the overall current can be summed as indicated.

In Eqs. (16)–(18),  $\bar{g}_1$  and  $\bar{g}_2$  represent the surface Green's functions for electrodes 1 and 2, respectively, when they are isolated.  $\bar{a}_1$  and  $\bar{a}_2$  are the corresponding spectral functions:  $\bar{a}_i = i(\bar{g}_i - \bar{g}_i^\dagger)$ . Each of these is represented by a  $2 \times 2$  Nambu matrix whose components are indicated by the superscripts  $ee$ ,  $eh$ ,  $he$ , and  $hh$ . If the expression for the surface Green's function is given for any unconventional superconductor, we can readily use Eqs. (16)–(18). In Appendix B1 we present a general method to obtain the surface Green's function of any unconventional superconductor. In this section we discuss only the cases for  $s$ -wave and  $d$ -wave symmetry. The surface Green's function for an  $s$ -wave superconductor is given by the standard BCS relation

$$\bar{g}_s(E) = \frac{-2i \sin^2 k_f a}{\hbar v_f} \begin{bmatrix} E & \Delta \\ \frac{E}{\sqrt{E^2 - \Delta^2}} & \frac{\Delta}{\sqrt{E^2 - \Delta^2}} \\ \Delta & E \\ \frac{\Delta}{\sqrt{E^2 - \Delta^2}} & \frac{E}{\sqrt{E^2 - \Delta^2}} \end{bmatrix}, \quad (19)$$

whereas the surface Green's function for a  $d$ -wave superconductor is given as (derived in Appendix B2)

$$\bar{g}_d(E, k_y) = \frac{2 \sin^2 k_f a}{\hbar v_f} \begin{bmatrix} -\cot k_f a - i \left( \frac{u_+ u_- + v_+ v_-}{u_+ u_- - v_+ v_-} \right) & -\frac{2i u_+ v_-}{u_+ u_- - v_+ v_-} \\ -\frac{2i v_+ u_-}{u_+ u_- - v_+ v_-} & \cot k_f a - i \left( \frac{u_+ u_- + v_+ v_-}{u_+ u_- - v_+ v_-} \right) \end{bmatrix}, \quad (20)$$

where  $u_\pm$  and  $v_\pm$  are defined as

$$u_\pm = u(\Delta_\pm) = e^{i\phi} \sqrt{(E + \sqrt{E^2 - |\Delta_\pm|^2})/2E}$$

and

$$v_\pm = v(\Delta_\pm) = \sqrt{(E - \sqrt{E^2 - |\Delta_\pm|^2})/2E}.$$

$\Delta_+$  and  $\Delta_-$  are the gaps in directions  $\alpha$  and  $-\alpha$ , where  $\alpha = \sin^{-1}(k_y/k_f)$  (see Fig. 5). If  $\Delta_+$  and  $\Delta_-$  have the same sign then the surface Green's function from Eq. (7) looks similar to that for an  $s$ -wave superconductor with two gaps  $\Delta_+$  and  $\Delta_-$ . But if  $\Delta_+$  and  $\Delta_-$  have opposite signs then the quantity  $(u_+ u_- - v_+ v_-)$  appearing in Eq. (20) vanishes for  $E=0$  giving rise to a singularity or ‘‘midgap peak.’’ In that case, close to  $E=0$ , we can write  $g$  from Eq. (20) approximately

as ( $\eta \approx \hbar/\tau_\phi$ ,  $\tau_\phi$ : dephasing time, we assume  $\Delta_+$  is positive and  $\Delta_-$  is negative without loss of generality)

$$\bar{g}_d(E \rightarrow 0, k_y) = \frac{4\bar{\Delta}(k_y) \sin^2 k_f a}{\hbar v_f (E + i\eta)} \begin{bmatrix} 1 & -i \\ i & 1 \end{bmatrix}, \quad (21)$$

where  $\bar{\Delta} = |\Delta_+| |\Delta_-| / (|\Delta_+| + |\Delta_-|)$  and the corresponding spectral function as

$$\bar{a}_d(E \rightarrow 0, k_y) = \frac{4\bar{\Delta}(k_y) \sin^2 k_f a}{\hbar v_f} \left( \frac{2\eta}{E^2 + \eta^2} \right) \begin{bmatrix} 1 & -i \\ i & 1 \end{bmatrix}. \quad (22)$$

*Josephson current.* By factoring out the phases of  $\bar{g}^{eh}$  and  $\bar{g}^{he}$ , Eq. (16) can be written as a sum of  $\sin(\phi_1 - \phi_2)$  and  $\cos(\phi_1 - \phi_2)$  components, where  $\phi_1$  and  $\phi_2$  are the phases of

the superconducting leads. Using the surface Green's function from Eqs. (19)–(22) in the sine component (the cosine component is usually zero), we have shown in Ref. 5 that the midgap contribution to the critical current at a Josephson junction between two  $d$ -wave superconductors with misorientations  $\theta_1$  and  $\theta_2$  has an orientation dependence of  $\sin 2\theta_1 \sin 2\theta_2$  that is exactly orthogonal to the Sigrist and Rice relation  $\cos 2\theta_1 \cos 2\theta_2$  commonly used to describe the orientation dependence of the Josephson current.<sup>34</sup> The midgap contribution to the Josephson current also has an anomalous temperature dependence that goes as  $1/T$ , which has been noted by a number of authors.<sup>5,6,35</sup> We can obtain this result analytically with a simple “back-of-the envelope” calculation from Eqs. (15) and (16), as shown earlier in Refs. 5,35. It is also evident from this calculation that the  $1/T$  increase in the Josephson current at low temperatures is ultimately limited by the value of  $\eta$  which is set by the dephasing processes.<sup>5</sup>

Note that if the intrinsic broadening  $\eta$  is very small, then the assumption that  $|Mg| \ll 1$  is violated even for small values of  $M$  due to the sharp singularity in  $g$ . It is then necessary to go to higher orders and the Josephson current will then contain significant contributions from the  $M^4$ ,  $M^6$  and higher terms, in addition to the usual  $M^2$  term considered here. Since the normal state resistance  $R_n$  remains proportional to  $M^2$ , we can expect that the  $I_c R_n$  product for such junctions will not be constant at low temperatures. Nonconstant  $I_c R_n$  products based on this mechanism should be distinguishable experimentally from those due to other causes through the temperature dependence.<sup>5</sup>

*Quasiparticle current.* The expression for the quasiparticle current  $i_{QP}$  [Eq. (17)] states that the current is proportional to the product of the surface DOS of the two electrodes, a fact that is commonly assumed by many experimentalists in interpreting their experimental data. However, an interesting consequence of midgap peaks that follows from Eq. (17) seems to have gone largely unnoticed. If we assume that electrode 1 is a superconductor with a midgap peak such that its DOS  $\equiv \delta(E)$ , then Eq. (16) predicts that the current should be given by

$$i_{QP} \approx [f(0) - f(V)] [a_2^{ee}(V)], \quad (23)$$

which is proportional to the DOS in electrode 2. This is very different from the usual situation where the differential conductance  $dI/dV$  is proportional to the DOS. Here the current itself (not the conductance) is proportional to the DOS. For example, if electrode 2 is a low- $T_c$  superconductor with a DOS having peaks at its superconducting gap, then the current will show peaks at these voltages implying a *negative* differential conductance. Whether such negative conductances will actually be observed in a given system depends on the sharpness of the midgap peak relative to the peak in the DOS of electrode 2. There is some experimental evidence for such negative conductances and a careful analysis of these anomalous results could help establish the reality of midgap peaks. Also since  $f(0) - f(V) \sim V/k_B T$ , we can expect the low bias conductance to scale inversely with temperature. Detailed calculations in Ref. 9 show that the  $I$ - $V$  characteristics for the  $s$ - $d_{xy}$  junction looks similar to the DOS of the  $s$ -wave superconductor and the  $I$ - $V$  characteris-

tics for the  $d_{x^2-y^2}$ - $d_{xy}$  junction looks similar to the DOS of a  $d_{x^2-y^2}$ -wave superconductor, both of which are in agreement with the previous discussion. Using the same argument one can show that the  $I$ - $V$  characteristics for  $d_{xy}$ - $d_{xy}$  junction should have a sharp peak near zero bias resulting in negative conductance. The scattering theory based calculation in Ref. 9 does not show this feature. The reason is that the scattering theory based calculation in Ref. 9 did not use any broadening so that the peak was infinitely sharp and easily missed. Since the experimental system has finite broadening, we believe this feature will show up in experimental system and may have already been seen in the measurements of Ref. 36.

*ac Josephson current.* The ac current between two  $d$ -wave superconductors [given by Eq. (18)] also has a strong peak near zero bias. This follows readily from Eq. (18), noting that the midgap singularities for superconductors 1 and 2 get progressively misaligned as the bias  $V$  is increased from zero. This strong bias dependence of the ac Josephson current is absent in  $s$ -wave superconductors and should provide convincing evidence for the presence of a singularity in the pair-correlation function. However this may be difficult to observe experimentally because of the high Josephson frequency  $\sim 1$  THz associated with a bias of  $\sim 1$  mV. As with the dc Josephson current, the peak decreases as  $\approx 1/T$ .

#### IV. NUMERICAL ILLUSTRATION: JOSEPHSON CURRENT OF STRONGLY COUPLED $d$ -WAVE JUNCTIONS

In the discussion of the previous section, we assumed that the tunneling matrix element  $M$  is small ( $|Mg| \ll 1$ ) and therefore we used a first-order theory. We also pointed out that due to sharp singularity in  $g$  originating from the midgap peak, this first-order theory may not hold if  $M/\eta \gg 1$ . One interesting consequence of the breakdown of first-order theory is the nonsinusoidal current phase  $[I(\phi)]$  relation. Such nonsinusoidal relations are well known for strongly coupled junctions, but when midgap peaks are involved it can arise even for weakly coupled junction. Recently it has become possible to directly probe the  $I(\phi)$  of Josephson junctions by applying a magnetic field.<sup>12,37</sup> The measurement of  $I(\phi)$  relation of bicrystal junctions between HTSC's (unpublished)<sup>12</sup> show nonsinusoidal behavior for some orientations of the  $d$ -wave order parameter and sinusoidal behavior for some other orientations suggesting that the nonsinusoidality may arise from some factor related to junction orientation rather than strong coupling. Since a first-order theory does not hold any more, in this section we present a calculation based on the full theory to show the nature of such nonsinusoidal behavior. This calculation also illustrates how the tight-binding parameters are chosen to represent a  $d$ -wave order parameter.

We compute the  $I(\phi)$  relation for a Josephson junction between two  $d$ -wave superconductors (Fig. 3). The superconductors are separated by a barrier of variable strength. To model the system shown in Fig. 3, we choose following  $H$ ,  $\mu$ ,  $U$ , and  $\Delta$  in Eq. (2).  $H$  is assumed to be the free-electron Hamiltonian

$$H = 2t[1 - \cos k_x a] + 2t[1 - \cos k_y a], \quad (24)$$

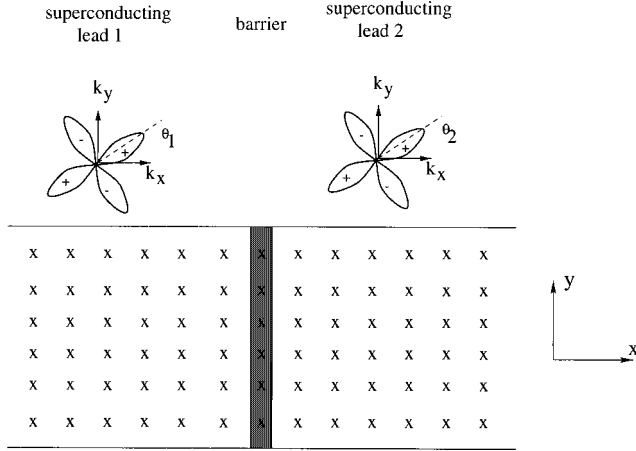


FIG. 3. Josephson junction between two  $d$ -wave superconductors with misorientation angles  $\theta_1$  and  $\theta_2$  separated by a barrier of variable strength. We model it in discrete space, where the structure is represented by set of lattice points marked as X in the figure. We assume the system to be translationally invariant in the  $y$  direction. The order parameters of the superconductors at the Fermi surface (in  $k$  space) are also shown.

$\mu$  is zero everywhere implying that the chemical potential is equal to  $\mu_F$ . The tunnel barrier is modeled using a uniform impurity layer of strength  $U_0$ . Also the order parameter is given as

$$\Delta = \begin{cases} \Delta_1 & \text{lead 1,} \\ 0 & \text{device,} \\ \Delta_2 & \text{lead 2,} \end{cases}$$

$$\Delta_i = \Delta_d e^{i\phi_i} [\cos 2\theta_i \{\cos k_y a - \cos k_x a\} + \sin 2\theta_i \sin k_x a \sin k_y a], \quad (25)$$

representing  $d$ -wave symmetry with misorientations  $\theta_i$  and phase  $\phi_i$ . The maximum gap value in Eq. (25) is  $\Delta_0 = \Delta_d \mu_F / t$ .  $H$  and  $\Delta$  in Eqs. (24) and (25) are given in the  $k$  space in a tight-binding form with minimum lattice spacing  $a$ .

In our computation, we discretize the system in the real space and represent the barrier by one layer (Fig. 3). Therefore the ‘‘effective device’’ (defined in Sec. II B) consists of three layers including one layer from each lead [ $1^*$ ,  $D$ ,  $2^*$ ]. Since we assume the system to be translationally invariant in the  $y$  direction,  $k_y$  is a good quantum number. Also at equilibrium different energies do not couple together. Therefore it is possible to compute the retarded Green’s function  $G_D$  separately for each individual  $E$  and  $k_y$ . To compute  $G_D$ , we first calculate the surface Green’s function  $g_{is}$  for lead  $i$  from Eqs. (7) and (8), where

$$\alpha_i = \begin{bmatrix} 4t - 2t \cos k_y a - \mu_F & \Delta_d \cos 2\theta_i \cos k_y a \\ \Delta_d \cos 2\theta_i \cos k_y a & -4t + 2t \cos k_y a + \mu_F \end{bmatrix},$$

and

$$\beta_i = \begin{bmatrix} -t & \frac{1}{2}(-\Delta_d \cos 2\theta_i - i \sin 2\theta_i \sin k_y a) \\ \frac{1}{2}(-\Delta_d \cos 2\theta_i - i \sin 2\theta_i \sin k_y a) & t \end{bmatrix}.$$

Since  $\mu$  is zero everywhere, the shifting described by Eq. (6) is not necessary. Once we have  $g_{is}$  for the leads,  $G_D$  is computed from Eq. (4) with

$$g_D = \begin{bmatrix} E - 4t + 2t \cos k_y a - U_0 + \mu_F & 0 \\ 0 & E + 4t - 2t \cos k_y a + U_0 - \mu_F \end{bmatrix}^{-1}$$

and

$$\tau_1 = \tau_2 = \begin{bmatrix} -t & 0 \\ 0 & t \end{bmatrix}.$$

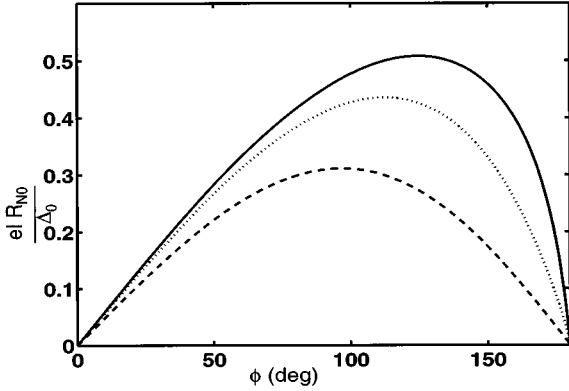
$\alpha_i$ ,  $\beta_i$ ,  $g_D$ ,  $\tau_1$ , and  $\tau_2$  given above are derived from the tight-binding forms of  $H$  and  $\Delta$  in Eqs. (24) and (25).<sup>38</sup>

At equilibrium, only the dc component [ $I_0$ ] of the current in Eq. (1) is nonzero and can be written as the sum of the components of current for each  $E$  and  $k_y$  value [combining Eqs. (9), (13), and (14)] as

$$I_0 = \frac{2et\Delta E}{hN_{k_y}} \sum_{E, k_y} \text{Re}[G_D(x_d, x_{1^*}, e, e) - G_D(x_{1^*}, x_d, e, e) + G_D(x_d, x_{1^*}, h, h) - G_D(x_{1^*}, x_d, h, h)] f(E), \quad (26)$$

where  $\Delta E = (E_{\max} - E_{\min})/N_E$  and  $N_{k_y}$  is the number of  $k_y$  points in the range  $(-k_F, k_F)$ , where  $k_F a = \cos^{-1}(1 - \mu_F/2t)$ .

(a)



(b)

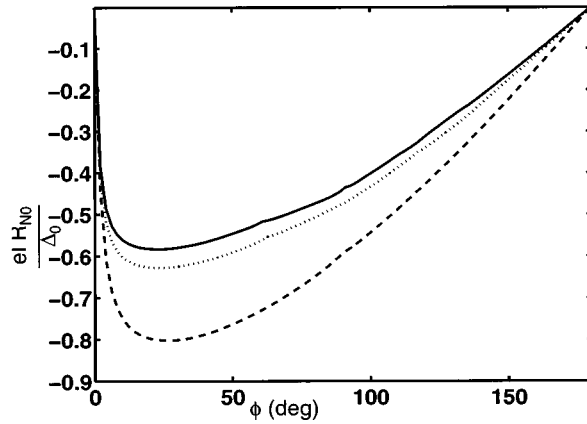


FIG. 4. Current-phase relation for the junction shown in Fig. 3 with (a)  $\theta_1 = \theta_2 = 0^\circ$  and (b)  $\theta_1 = 45^\circ$  and  $\theta_2 = -45^\circ$ . The three plots are for different barrier strengths (solid:  $T_0 = 1$ , dotted:  $T_0 = 0.9$ , dashed:  $T_0 = 0.5$ ). The other parameters in our computation are  $\mu_F/t = 1.5$  and  $\Delta_d/t = 0.05$ .

In this paper, we plot  $eIR_{N0}/\Delta_0$  vs  $\phi$  for  $T_0 = 1, 0.9, 0.5$ , where  $T_0$  represents the barrier transmission probability in the direction normal to the junction.  $U_0$  and  $R_{N0}$  are directly related to  $T_0$  given by  $T_0 = [\{U_0/2t \sin k_f a\}^2 + 1]^{-1}$  and  $R_{N0} = h/2e^2 T_0$ . Two possible orientations of the order parameter are shown [ $\theta_1 = \theta_2 = 0^\circ$  in Fig. 4(a) and  $\theta_1 = 45^\circ$  and  $\theta_2 = -45^\circ$  in Fig. 4(b)].

Several features of the plots are discussed below: (i) When the barrier is low ( $T \approx 1$ ),  $I(\phi)$  is nonsinusoidal with a current changing sign rapidly at  $\phi = \pi$  in Fig. 4(a) and at  $\phi = 0$  in Fig. 4(b). The nonsinusoidal behavior in Fig. 4(a) with a change of the sign of current at  $\phi = \pi$  can be predicted by straightforwardly extending the previous theories for strongly coupled  $s$ -wave superconductors<sup>16</sup> but the nonsinusoidal behavior in Fig. 4(b) is usual for  $d$ -wave superconductors. The extra  $\pi$  phase shift in this case occurs due to the formation of  $\pi$  junction for this orientation. Experimental measurements of  $I(\phi)$  for bicrystal junctions between HTSC's show similar behavior for certain orientations of the superconductors.<sup>12</sup> (ii) Although  $I_c R_n$  is constant in the tunneling limit,<sup>5,33</sup> it does not remain constant when the barrier gets lower. This is because in the tunneling limit terms only with the lowest order of the coupling strength contribute to

the current,<sup>5</sup> but when the coupling is higher, the higher-order terms also become significant leading to nonconstant  $I_c R_n$ . Experimental observation of nonconstant  $I_c R_n$  in grain-boundary bicrystal junctions between HTSC's suggests that they may be modeled as strongly coupled junctions. (iii) As the coupling becomes weaker (smaller  $T$ ),  $I(\phi)$  turns more sinusoidal for the junction with  $\theta_1 = \theta_2 = 0^\circ$ , but for the junction with  $\theta_1 = 45^\circ$  and  $\theta_2 = -45^\circ$  the introduction of the barrier results in formation of midgap states.<sup>1,2</sup> The resulting singularity in  $g$  makes the product  $Mg$  large so that the  $I(\phi)$  remains nonsinusoidal even for small  $M$ . This effect should be observable if  $M\eta \gg 1$ . Experimentally some orientations of the bicrystal junctions have been reported to show more pronounced nonsinusoidal behavior than other orientations<sup>12</sup> which may be explained by the above observation.

## V. CONCLUSION

In this paper, we presented a general and powerful numerical method to model transport experiments between unconventional superconductors. The method in its general form is discussed in Sec. II and specific cases are considered in Secs. III and IV. By using the surface Green's functions in the expressions instead of the bulk Green's functions, our method correctly accounts for the surface effects such as midgap states predicted for  $d$ -wave superconductors.<sup>1-9</sup> Our method does not make the quasiclassical approximation used in the quasiclassical Green's function method. The choice of the tight-binding description enables our method to include any unconventional order parameter and arbitrary band structures and therefore makes it more versatile than the scattering theory.

The Green's-function-based description has another advantage over scattering theory. The expressions from our method simplify significantly for weakly coupled "tunnel" junctions. Such weakly coupled junctions have been studied extensively in the context of low- $T_c$  superconductors, but in the present context they are particularly relevant. This is because the effect of the midgap states is most prominent for weakly coupled junctions,<sup>2</sup> whose  $I$ - $V$  characteristics can be modeled with a much simpler first-order theory that provides greater insight than a purely numerical calculation based on the full theory.<sup>9</sup> In Sec. III such a first-order theory for the dc Josephson current, the ac Josephson current, and the quasiparticle current is presented, which could be described as a generalized tunneling Hamiltonian formalism. Several results and insights are derived from these expressions.

In addition to the tunneling limit, our method can also be used to describe junctions with arbitrary coupling. In Sec. IV we illustrated this by computing the current-phase [ $I(\phi)$ ] relation for a junction between two  $d$ -wave superconductors with arbitrary coupling. Unlike the  $I(\phi)$  in  $s$ -wave junctions that changes from nonsinusoidal to sinusoidal dependence when the junction coupling is reduced, for some orientations of the  $d$ -wave order parameter nonsinusoidal nature of  $I(\phi)$  is maintained even at low coupling. Some evidence of similar behavior has been seen experimentally (unpublished<sup>12</sup>) and our theory could provide motivation for further experiments in this direction.

### ACKNOWLEDGMENTS

We acknowledge useful discussions with H. Hilgenkamp and I. Il'ichev. We are grateful to P. F. Bagwell and R. Riedel for drawing our attention to the nonsinusoidal current-phase relation for certain  $d$ -wave orientations. We also thank Husrev Tolga Ilhan for a critical reading of the manuscript. The work was supported by the MRSEC program of the National Science Foundation under Award No. DMR-9400415.

### APPENDIX A: TUNNELING LIMIT EXPANSION

In this appendix, starting from the general formulation discussed in Sec. II, we derive simple expressions for the dc and ac components of current for tunnel junctions between unconventional superconductors. In Sec. II, we represented the system on a tight-binding lattice and computed Green's function for an "effective device" consisting of the normal device region and one point from each superconducting lead. The "effective device" we consider in this specific case consists of two points—one representing each superconducting lead. Since the device is short, we do not consider any point in the device region. We also assume the system to be uniform in the transverse ( $y$ ) direction resulting in decoupling of different  $k_y$  values. For each  $k_y$ , we have a one-dimensional "effective device" consisting of two lattice points connected by a matrix element  $M(k_y)$ .

The retarded Green's function for this two-point device can be written from Eq. (4) as

$$G_D(E, k_y) = \begin{bmatrix} g_1^{-1} & -(M) \\ -(M^\dagger) & g_2^{-1} \end{bmatrix}^{-1} \approx \begin{bmatrix} g_1 & g_1 M g_2 \\ g_2 M^\dagger g_1 & g_2 \end{bmatrix}. \quad (\text{A1})$$

$g_1$  and  $g_2$  are the surface Green's functions of the semi-infinite leads that can be computed from Eqs. (7) and (8) using the procedure described in Sec. B 1. In Eq. (A1) we performed a perturbation expansion in powers of  $M$  and kept only the terms first order in  $M$ . This is valid when the coupling  $M$  is small ( $|M g_i| \ll 1$ ) indicating a large barrier between the superconductors.

The current between the superconductors is expressed in terms of  $G^<$ . Using Eqs. (10), (11), and (A1),  $G^<$  can be written as

$$G^< = G_D \begin{bmatrix} \sigma_1^< & 0 \\ 0 & \sigma_2^< \end{bmatrix} G_D^\dagger = \begin{bmatrix} \alpha_1 & \alpha_1 M g_2^\dagger + g_1 M \alpha_2 \\ g_2 M^\dagger \alpha_1 + \alpha_2 M^\dagger g_1^\dagger & \alpha_2 \end{bmatrix}, \quad (\text{A2})$$

where  $\alpha_i = g_i \sigma_i^< g_i^\dagger = \alpha_i^\dagger$ .  $\sigma_1$  and  $\sigma_2$  are the pair-correlation functions of the individual superconducting leads that include the effects of their potentials as given by Eq. (12).

Different components of the current can be obtained as diagonal and off-diagonal parts of the current operator. The current operator  $I_{\text{OP}}$  is a matrix of size  $2N_E$  given by

$$I_{\text{OP}} = \frac{e}{h} [(M g_2 M^\dagger \alpha_1 + M \alpha_2 M^\dagger g_1^\dagger - M^\dagger \alpha_1 M g_2^\dagger - M^\dagger g_1 M \alpha_2)] = \frac{e}{h} |M(k_y)|^2 [(\tau_3 g_2 \tau_3 \alpha_1 + \tau_3 \alpha_2 \tau_3 g_1^\dagger - \tau_3 \alpha_1 \tau_3 g_2^\dagger - \tau_3 g_1 \tau_3 \alpha_2)]. \quad (\text{A3})$$

$\tau_3$  is the Pauli matrix in electron-hole space (diagonal matrix with 1 for the electron component and  $-1$  for the hole component). Expressing all the functions in the current operator in terms of the functions in the untransformed domain, we obtain Eqs. (15)–(18) for the components of current.<sup>38</sup> The transformation of  $g$  is shown in Eq. (6), from which the following transformation of  $\alpha$  is derived. Since in the untransformed domain

$$\bar{\alpha}_i = \bar{g}_i \bar{\sigma}_i^< \bar{g}_i^\dagger = i f(E) \bar{a}_i(E), \quad (\text{A4})$$

where  $\bar{a} = i(\bar{g} - \bar{g}^\dagger)$  is the spectral function, and the transformations of different components of  $\alpha$  are

$$\begin{aligned} \alpha_i^{ee}(E', E) &= i \delta_{E', E} \bar{a}_i^{ee}(E - \mu_i) f(E - \mu_i) \\ &= i \delta_{E', E} \bar{a}_i^{ee}(E' - \mu_i) f(E' - \mu_i), \end{aligned}$$

$$\begin{aligned} \alpha_i^{eh}(E', E) &= i \delta_{E', E+2\mu_i} \bar{a}_i^{eh}(E + \mu_i) f(E + \mu_i) \\ &= i \delta_{E', E+2\mu_i} \bar{a}_i^{eh}(E' - \mu_i) f(E' - \mu_i), \end{aligned}$$

$$\begin{aligned} \alpha_i^{he}(E', E) &= i \delta_{E', E-2\mu_i} \bar{a}_i^{he}(E - \mu_i) f(E - \mu_i) \\ &= i \delta_{E', E-2\mu_i} \bar{a}_i^{he}(E' + \mu_i) f(E' + \mu_i), \end{aligned}$$

$$\begin{aligned} \alpha_i^{hh}(E', E) &= i \delta_{E', E} \bar{a}_i^{hh}(E + \mu_i) f(E + \mu_i) \\ &= i \delta_{E', E} \bar{a}_i^{hh}(E' + \mu_i) f(E' + \mu_i). \end{aligned}$$

### APPENDIX B: SURFACE GREEN'S FUNCTION

In order to apply the method presented in Sec. II to any unconventional superconductor we need to have either a numerical method for solving Eqs. (7) and (8) from given  $E$ ,  $\alpha_i$ , and  $\beta_i$  matrices or analytical expressions for the surface Green's functions. In Sec. B 1 we present a general numerical method for solving Eqs. (7) and (8) that can be applied for any unconventional superconductor with arbitrary pairing symmetry and band structure. Since  $d$ -wave superconductors are more commonly used, in Sec. B 2 we derive exact analytical expressions (valid within the Andreev approximation  $\mu \ll \Delta$ ) for the surface Green's functions of  $d$ -wave superconductors. The method of Sec. B 2 can also be extended to obtain analytical expressions of surface Green's function for other unconventional superconductors, but arbitrary band structure cannot be easily included due to difficulty in obtaining the expressions for eigenstates in such cases.

### 1. Numerical method

In order to obtain the surface Green's function  $\bar{g}_i(E)$  of lead  $i$  from given  $E$ ,  $\alpha_i$ , and  $\beta_i$ , we solve Eqs. (7) or (8) using an iterative procedure. We start with some  $\bar{g}^0$  as the initial guess on the right-hand side (RHS) and compute the left-hand side (LHS) [ $\bar{g}^{\text{temp}}$ ]. In the next iteration we use  $(\bar{g}^0 + \bar{g}^{\text{temp}})/2$  on the RHS. The iterations are continued until convergence is reached. If we use nonzero  $\eta$  while solving Eqs. (7) and (8), the rate of convergence improves at the cost of accuracy. Choice of initial  $\bar{g}^0$  is arbitrary except that it needs to have a positive complex part in order to converge to the retarded Green's function. In our computation we choose  $\bar{g}^0 = \alpha + 0.0005iI$  as the initial guess.

A similar iterative procedure can be used to compute the bulk Green's function. In this case, we need to consider an infinite lead instead of the semi-infinite one shown in Fig. 2. An infinite region can be conceptually broken into two separate semi-infinite regions ( $L$  and  $R$ ), for which the surface Green's functions ( $\bar{g}_L$  and  $\bar{g}_R$ ) are computed using the procedure outlined above. Once  $\bar{g}_L$  and  $\bar{g}_R$  are known, the bulk Green's function is computed from

$$\bar{g}_{\text{bulk}}(E) = [(E + i\eta)I - \alpha - \beta^\dagger \bar{g}_L(E) \beta - \beta \bar{g}_R(E) \beta^\dagger]^{-1}_{\eta \rightarrow 0}. \quad (\text{B1})$$

The method presented here is general and can be used for any unconventional superconductor with arbitrary band structure and pairing symmetry. Given any unconventional band structure and pairing symmetry, we can obtain the equivalent  $\alpha$  and  $\beta$  matrices from the tight-binding representation and then we can use the method presented above.

### 2. Analytical expression based on scattering theory

Although the numerical method presented in Sec. B 1 can be used for any unconventional pairing symmetry, we believe that use of analytical expressions for simple cases provides better understanding of the behavior. In this section we derive analytical expressions for the surface and the bulk Green's functions for  $d$ -wave symmetry (within the limits of Andreev approximation  $\mu \gg \Delta$ ). The method presented here is fairly general and can be used for other types of unconventional superconductors.

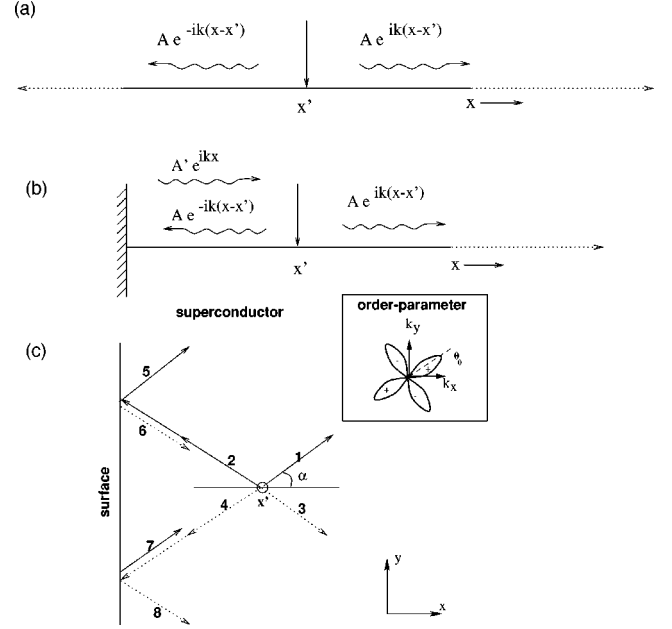


FIG. 5. (a) An impulse excitation in an infinite metal at point  $x'$  gives rise to outgoing waves  $A e^{ik(x-x')}$  in the region  $x > x'$  and  $A e^{-ik(x-x')}$  in the region  $x < x'$ . (b) In a semi-infinite metal, the wave traveling from the impulse source in the direction  $x < x'$  gets reflected from the boundary and modifies the total wave amplitudes at different points. (c) We compute the surface and the bulk density of states of a planar superconducting region. The order parameter in the superconductor (in  $k$  space) has  $d$ -wave symmetry with misorientation angle  $\theta$ . The figure also shows the quasiexcitations generated from an impulse at point  $x'$  in the superconductor. Solid lines show the propagation of the electronlike excitations 1,2,5,7 and dotted lines show the propagation of the holelike excitations 3,4,6,8. The figure also shows the quasiexcitations reflected from the surface.

We consider a planar superconducting region as shown in Fig. 5(c). We assume that the translational symmetry is preserved in the transverse ( $y$ ) direction. Therefore  $k_y$  is conserved and we can treat each  $k_y$  independently. The retarded Green's function of the superconductor for given  $E$  and  $k_y$  [ $G(E, k_y, x, x')$ ] is obtained from the Bogoliubov–de Gennes Hamiltonian<sup>26</sup>

$$\begin{bmatrix} \left( E + \frac{\hbar^2}{2m} \frac{\partial^2}{\partial x^2} - \frac{\hbar^2 k_y^2}{2m} + \mu \right) & -\Delta \\ -\Delta^\dagger & \left( E - \frac{\hbar^2}{2m} \frac{\partial^2}{\partial x^2} + \frac{\hbar^2 k_y^2}{2m} - \mu \right) \end{bmatrix} \begin{bmatrix} G^{ee}(E, k_y, x, x') & G^{eh}(E, k_y, x, x') \\ G^{he}(E, k_y, x, x') & G^{hh}(E, k_y, x, x') \end{bmatrix} \\ = \begin{bmatrix} \delta(x-x') & 0 \\ 0 & \delta(x-x') \end{bmatrix}. \quad (\text{B2})$$

Physically Eq. (B2) describes the motion of electronlike and holelike quasiparticles coupled together by the order parameter  $\Delta$ . We choose  $\Delta$  with  $d$ -wave symmetry having the following directional dependence in  $k$  space:  $\Delta(\theta) = \Delta_0 \cos(2\theta - 2\theta_0)$ , where  $\theta$  is the orientation with respect to the  $k_x$  axis [Fig. 5(c)].

To obtain the Green's function from the scattering picture, we consider the propagation of the quasiexcitations generated from an impulse. Two columns of the Green's function matrix in Eq. (B2) are obtained by considering the wave amplitude at point  $x$  due to electronlike impulse  $\{[\delta(x-x') \ 0]'\}$  and holelike impulse  $\{[0 \ \delta(x-x')]\}'$  separately. For any chosen values of  $E$  and  $k_y$ , an impulse gives rise to four possible excitations—electronlike excitation propagating in directions 1 and 2 and holelike excitations propagating in directions 3 and 4 [Fig. 5(c)]. These quasiexcitations propagate having angle  $\alpha$  with the  $x$  axis, where  $\alpha = \sin^{-1}(k_y/k_f)$  [ $k_f = \sqrt{2m\mu/\hbar^2}$ ]. Each propagating mode experiences order parameters in its direction of propagation. Therefore propagating modes in directions 1 and 4 experience order parameters  $\Delta_+ = \Delta(\alpha)$  and propagating modes in directions 2 and 3 experience order parameters  $\Delta_- = \Delta(-\alpha)$ . For an  $s$ -wave superconductor with order parameter  $\Delta = |\Delta|e^{i\phi}$  and  $\Delta \ll \mu$ ,<sup>39</sup> the propagating modes at an energy  $E$  are  $[u(\Delta) \ v(\Delta)]^T e^{\pm ik_f(x-x')}$  (electronlike excitation) and  $[v(\Delta) \ u(\Delta)]^T e^{\mp ik_f(x-x')}$  (holelike excitation) for  $x > (<)x'$ , where  $u(\Delta) = e^{i\phi} \sqrt{(E + \sqrt{E^2 - |\Delta|^2})/2E}$ ,  $v(\Delta) = \sqrt{(E - \sqrt{E^2 - |\Delta|^2})/2E}$  and  $k \approx k_f = \sqrt{2m\mu/\hbar^2}$ .<sup>16</sup> For the  $d$ -wave superconductor under consideration different wave components can be written in terms of the  $u$  and  $v$ 's in those

particular directions. Here we discuss the propagating waves for only the electronlike excitation. The wave functions for  $x > x'$  and for  $x < x'$  are given as

$$\Psi^+ = \alpha_1 e^{ik(x-x')} \begin{bmatrix} u_+ \\ v_+ \end{bmatrix} + \alpha_2 e^{-ik(x-x')} \begin{bmatrix} v_- \\ u_- \end{bmatrix} \quad (\text{B3})$$

and

$$\Psi^- = \alpha_3 e^{-ik(x-x')} \begin{bmatrix} u_- \\ v_- \end{bmatrix} + \alpha_4 e^{ik(x-x')} \begin{bmatrix} v_+ \\ u_+ \end{bmatrix}, \quad (\text{B4})$$

where  $u, v_{\pm} = u, v(\Delta_{\pm})$ . By matching boundary condition at  $x = x'$ , we get

$$\alpha_1 = (u_+ / i\hbar v_x) (E / \sqrt{E^2 - |\Delta_+|^2}),$$

$$\alpha_2 = (v_- / i\hbar v_x) (E / \sqrt{E^2 - |\Delta_-|^2}),$$

$$\alpha_3 = (u_- / i\hbar v_x) (E / \sqrt{E^2 - |\Delta_-|^2})$$

and

$$\alpha_4 = v_+ / (u_+^2 - v_+^2) = (v_+ / i\hbar v_x) (E / \sqrt{E^2 - |\Delta_+|^2}).$$

This allows us to get the first column of the bulk Green's-function matrix. Similarly the second column of the bulk Green's-function matrix can be obtained by considering the propagations of waves generated by a holelike impulse. Combining them, the bulk Green's function can be written as

$$g^{\text{bulk}} = \frac{1}{2i\hbar v_f} \begin{bmatrix} \frac{E}{\sqrt{E^2 - \Delta_+^2}} + \frac{E}{\sqrt{E^2 - \Delta_-^2}} & \frac{\Delta_+}{\sqrt{E^2 - \Delta_+^2}} + \frac{\Delta_-}{\sqrt{E^2 - \Delta_-^2}} \\ \frac{\Delta_+}{\sqrt{E^2 - \Delta_+^2}} + \frac{\Delta_-}{\sqrt{E^2 - \Delta_-^2}} & \frac{E}{\sqrt{E^2 - \Delta_+^2}} + \frac{E}{\sqrt{E^2 - \Delta_-^2}} \end{bmatrix}.$$

To obtain the surface Green's function, we need to consider the reflection of the waves from the surface. In Fig. 5(c), we have shown the reflection of electronlike excitation 2 [ $e^{-ikx}(u_- \ v_-)^T$ ] into electronlike 5 [ $e^{ikx}(u_+ \ v_+)^T$ ] and holelike 6 [ $e^{-ikx}(v_- \ u_-)^T$ ]:

$$e^{-ikx} \begin{bmatrix} u_- \\ v_- \end{bmatrix} \rightarrow a e^{ikx} \begin{bmatrix} u_+ \\ v_+ \end{bmatrix} + b e^{-ikx} \begin{bmatrix} v_- \\ u_- \end{bmatrix}, \quad (\text{B5})$$

where  $a = -(u_-^2 - v_-^2)/(u_+ u_- - v_+ v_-)$  and  $b = -(v_- u_+ - u_- v_+)/ (u_+ u_- - v_+ v_-)$  and the reflection of holelike 4

[ $e^{ikx}(v_+ \ u_+)^T$ ] into electronlike 7 [ $e^{ikx}(u_+ \ v_+)^T$ ] and holelike 8 [ $e^{-ikx}(v_- \ u_-)^T$ ]:

$$e^{ikx} \begin{bmatrix} v_+ \\ u_+ \end{bmatrix} \rightarrow c e^{-ikx} \begin{bmatrix} v_- \\ u_- \end{bmatrix} + d e^{ikx} \begin{bmatrix} u_+ \\ v_+ \end{bmatrix}, \quad (\text{B6})$$

where  $c = -(u_+^2 - v_+^2)/(u_+ u_- - v_+ v_-)$  and  $d = -(v_+ u_- - u_+ v_-)/(u_+ u_- - v_+ v_-)$ . Combining the contributions of all waves,<sup>38</sup> Eq. (20) for the surface Green's function can be written.

\*Present address: Hewlett-Packard Company, 1501 Page Mill Road, MS-6LC, Palo Alto, CA 94304-1126.

<sup>1</sup>C. R. Hu, Phys. Rev. Lett. **72**, 1526 (1994); J. Yang and C. R. Hu, Phys. Rev. B **50**, R16 766 (1994).

<sup>2</sup>Y. Tanaka and S. Kashiwaya, Phys. Rev. Lett. **74**, 3451 (1995); S. Kashiwaya, Y. Tanaka, M. Koyanagi, and K. Kajimura, Phys. Rev. B **53**, 2667 (1996).

<sup>3</sup>M. Matsumoto and H. Shiba, J. Phys. Soc. Jpn. **64**, 3384 (1995); **64**, 4867 (1995); **65**, 2194 (1996).

<sup>4</sup>Y. Tanaka and S. Kashiwaya, Phys. Rev. B **53**, R11 957 (1996).

<sup>5</sup>M. P. Samanta and S. Datta, Phys. Rev. B **55**, R8689 (1997).

<sup>6</sup>Y. S. Barash, H. Burkhardt, and D. Rainer, Phys. Rev. Lett. **77**, 4070 (1996).

<sup>7</sup>M. Fogelström, D. Rainer, and J. A. Sauls, Phys. Rev. Lett. **79**, 281 (1997).

<sup>8</sup>Y. Tanaka and S. Kashiwaya, Phys. Rev. B **56**, 892 (1997), and references therein.

<sup>9</sup>M. Hurd, Phys. Rev. B **55**, R11 993 (1997).

<sup>10</sup>J. R. Kirtley *et al.*, Phys. Rev. Lett. **76**, 1336 (1996); J. R. Kirtley

- et al.*, Nature (London) **373**, 225 (1995); C. C. Tsuei *et al.*, Science **271**, 329 (1996).
- <sup>11</sup>This nonsinusoidal behavior was pointed out to us by our colleagues R. A. Riedel and P. F. Bagwell (unpublished).
- <sup>12</sup>E. V. Il'ichev (private communication); V. Zakosarenko, E. V. Il'ichev, R. P. J. Ijsselsteijn, and V. Schultze, IEEE Trans. Appl. Supercond. **7**, 1057 (1997); E. Il'ichev, V. Zakosarenko, R. P. J. Ijsselsteijn, and V. Schultze, J. Low Temp. Phys. **106**, 503 (1997).
- <sup>13</sup>G. E. Blonder, M. Tinkham, and T. M. Klapwijk, Phys. Rev. B **25**, 4515 (1982).
- <sup>14</sup>M. Octavio *et al.*, Phys. Rev. B **27**, 6739 (1983).
- <sup>15</sup>T. M. Klapwijk *et al.*, Physica B **109 & 110**, 1657 (1982).
- <sup>16</sup>P. F. Bagwell, Phys. Rev. B **46**, 12 573 (1992), and references therein.
- <sup>17</sup>D. Averin and A. Bardas, Phys. Rev. Lett. **75**, 1831 (1995), and references therein.
- <sup>18</sup>S. Datta, P. F. Bagwell, and M. P. Anantram, Phys. Low-Dimens. Semicond. Struct. **3**, 1 (1996).
- <sup>19</sup>G. B. Arnold, J. Low Temp. Phys. **59**, 143 (1985).
- <sup>20</sup>J. C. Cuevas, A. M. Rodero, and A. L. Yeyati, Phys. Rev. B **54**, 7366 (1996).
- <sup>21</sup>S. Datta, *Electronic Transport in Mesoscopic Systems* (Cambridge University Press, Cambridge, 1995).
- <sup>22</sup>L. J. Buchholtz, M. Palumbo, D. Rainer, and J. A. Sauls, J. Low Temp. Phys. **101**, 1099 (1995); **101**, 1079 (1995).
- <sup>23</sup>C. Bruder, Phys. Rev. B **41**, 4017 (1990).
- <sup>24</sup>S. Yip, Phys. Rev. B **52**, 3087 (1995).
- <sup>25</sup>A. V. Zaitsev, Zh. Eksp. Teor. Fiz. **86**, 1742 (1984) [Sov. Phys. JETP **59**, 1015 (1984)].
- <sup>26</sup>P. G. de Gennes, *Superconductivity of Metals and Alloys* (Benjamin, New York, 1966), Chap. 5.
- <sup>27</sup>L. V. Keldysh, Sov. Phys. JETP **20**, 1018 (1965).
- <sup>28</sup>See, for example, R. J. Radtke, S. Ullah, K. Levin, and M. R. Norman, Phys. Rev. B **46**, 11 975 (1992).
- <sup>29</sup>M. Hurd, S. Datta, and P. F. Bagwell, Phys. Rev. B **54**, 6557 (1996).
- <sup>30</sup>C. Caroli, R. Combescot, P. Nozieres, and D. Saint-James, J. Phys. C **4**, 4854 (1971).
- <sup>31</sup>To derive Eq. (4) from Eq. (3), we need to write the Hamiltonian in Eq. (3) in terms of different layers of the system. Derivation for normal system is outlined in Chap. 3 of Ref. 21. We modify it to apply it for superconductors.
- <sup>32</sup>We derive the current operator by generalizing the method used in Ref. 30 for normal conductors.
- <sup>33</sup>V. Ambegaokar and A. Baratoff, Phys. Rev. Lett. **10**, 486 (1963); **11**, 104 (1963).
- <sup>34</sup>M. Sigrist and T. M. Rice, J. Phys. Soc. Jpn. **61**, 4283 (1992); Rev. Mod. Phys. **67**, 503 (1995).
- <sup>35</sup>S. Datta and M. P. Samanta, cond-mat/9606065 (unpublished).
- <sup>36</sup>H. Hancotte *et al.*, Phys. Rev. B **55**, R3410 (1997).
- <sup>37</sup>M. C. Koops, G. V. van Duyneveldt, and R. de Bruyn Ouboter, Phys. Rev. Lett. **77**, 2542 (1996).
- <sup>38</sup>M. P. Samanta and S. Datta (unpublished).
- <sup>39</sup>Only in this derivation, we use Andreev approximation [ $k \approx k_f = \sqrt{2m\mu/\hbar^2}$ ]. This approximation is valid for all energies close to the superconducting gap, when  $\Delta \ll \mu$  (Ref. 16) and therefore may not always be applicable. For more accurate results, one should use the numerical method discussed in Appendix B1.